MATERIALE PLASTICE
https://revmaterialeplastice.ro
https://doi.org/10.37358/Mat.Plast.1964

Characterization of Some Functional Polymeric Composites in a Synergistic Regime of Protection at Electromagnetic Shielding and Electrostatic Transfer

ALINA RUXANDRA CARAMITU[1], IOANA ION[1], MIHAI MARIN[1], ADRIANA MARIANA BORS[2*], ROMEO CRISTIAN CIOBANU[3], CRISTINA SCHREINER[3], MIHAELA ARADOAEI[3]

[1] National Institute for Research and Development in Electrical Engineering ICPE - CA Bucharest, 313 Splaiul Unirii, 030138, Bucharest, Romania
[2]INOE 2000-IHP, General Hydraulics Department, 14 Cutitul de Argint Str., 040558, Bucharest, Romania
[3] Gheorghe Asachi Technical University, Department of Electrical Measurements and Materials, 67 Dimitrie Mangeron Blvd., 700050, Iasi, Romania

Abstract: *The paper presents the characterization of 5 polymer composite materials with a polypropylene (PP) matrix obtained with different (mass) concentrations of strontium ferrite ($Fe_{12}SrO_{19}$) reinforcement that have synergistic protective properties against electrostatic discharges (ESD) and electromagnetic impulses (EMI). These types of composites can be used to protect electronic equipment. To this purpose, suitable polymer composites were developed using $SrFe_{12}O_{19}$ type filler in two forms (powder and concentrate). The weight ratio of the PP/$SrFe_{12}O_{19}$ composites obtained by the extrusion process and injection from the melt is 75/25 and 70/30. The characterization of these composite materials consisted of carrying out some physico-chemical tests to determine the hydrostatic density and the resistance to the action of water, as well as FTIR, UV-Vis analyzes and dielectric, magnetic and functional tests to identify the simultaneous protection performance at electromagnetic shielding and electrostatic discharges, which can occur in the electro-technical, electronics and automotive industries. It is also found that all composite materials presented reflection shielding properties (SER) in the range: -71.5 dB...to -56.7 dB, indicating very low absorption shielding. The best performing material was the PP/$SrFe_{12}O_{19}$ powder composite with a weight ratio of 70/30. At the same time, EDS tests were also carried out on these materials. For these applications, the surface resistance Rs and the point-to-point resistance Rp were tested. Recommended composites for simultaneous EMI and sensitivity to electrostatic discharges (ESD) functionality, in order of their performance, are M2 (with 30% ferrite powder) and M1 (with 25% ferrite powder). M4 composite (with 30% ferrite powder concentrate) can also be used at the limit. Following the research carried out, the obtained results recommend the composite with promising simultaneous operations as M2 (with 30% ferrite powder). The element of originality consists of obtaining polymer composites with simultaneous properties of protection against electromagnetic impulses and electrostatic discharges.*

Keywords*: strontium ferrite, PP/ $SrFe_{12}O_{19}$, polymer composites, electromagnetic radiation, magnetic permeability, electro-static discharge (ESD), electromagnetic impulses (EMI)*

1. Introduction

Radio waves, television waves, microwaves, X-rays, visible light waves are all examples of electromagnetic waves [1, 2], they differ from each other only in wavelength or frequency. High-frequency electromagnetic waves (MHz, GHz) transmitted by electronic equipment such as microwave oven, antennas for 4G, 5G mobile communications, etc. have a harmful effect on the health of plants, animals and people because these waves applied at high frequencies decrease the resistance of animal and human organism leading to the appearance of various diseases and even death [2, 3]. Therefore, exposure to electromagnetic waves must be minimized by shielding them with different composite shielding materials [4, 5]. The continuous increase in electricity production due to the ever-increasing

**email: bors.ihp@fluidas.ro*

demand of consumers, which generates electromagnetic fields, leads to an increase in electromagnetic pollution of the environment in various rooms/spaces/deposits/offices [6].

At the same time, all electronic devices, which have become so indispensable in everyday life, induce an increased sensitivity to electrostatic discharges (ESD), which imposes finding new, high-performance materials to ensure protection against these discharges [7-10]. Electromagnetic and electrostatic pollution, constantly increasing, can lead to the deterioration of human health [11-13] and living matter [14-21], so it is impetuously necessary to reduce it by researching and designing different new materials, effective for this purpose. These materials must simultaneously ensure an acceptable attenuation of electromagnetic waves, as well as a protection against electrostatic discharges as a result of phenomena associated with other local contaminations on humans and the environment [22, 23].

The usual filler materials for the realization of composite materials used as protective shields for electromagnetic waves are metal powders [24] or ferrite powders at sizes below 30 nm [25, 26], which present exceptional shielding properties. Over the years, there have been researches carried out to obtain composite materials using rubber as a polymer matrix [27] and Cr and Mn ferrite filler, materials that find their utility in absorbing microwaves in the 8-12 GHz range, at the same time, a silicone/ NiCr0.2Fe1.8O type composite was obtained for use in obtaining permanent magnets [28].

Most of the research carried out so far on these composite materials has been carried out in order to diversify the performances of permanent magnets. Research in terms of finding new composite materials that simultaneously fulfil the condition for electromagnetic shielding, but also as protection against electrostatic discharges, has not been carried out. That's why, in this work, we set out to obtain and characterize polymeric composites of the PP/$Fe_{12}SrO_{19}$ type with simultaneous applications in the protection against electromagnetic impulses and electrostatic discharges from electronic devices existing in the electro-technical, electronics and automotive industries. Thus, in the paper also presented the results obtained in the ESD functional tests that qualify the composites that simultaneously meet the conditions of protection and both to electromagnetic impulses and to electrostatic discharges.

The characterization of these materials consisted in performing dielectric tests, tests to determine the magnetic permeability with the estimation, by calculation, of the electromagnetic shielding efficiency and functional tests for ESD applications. As a result of these researches, it has been demonstrated that polymer composite materials (thermoplastics) with superior simultaneous EMI and ESD shielding properties can be obtained. These composites are easy to make on a large scale, cheap, with minimal concentration in ferrite powder type filler, but mostly they are easy-to-process thermoplastic materials for applications in the electrical, electronics and automotive industries.

2. Materials and methods

The following raw materials were used to obtain polymer composite materials:

- Polypropylene polymer matrix - RESINEX with the code PP RXP 2004 NATURAL (PP/25/1300 μm) [29]. Its characteristics are presented in Table 1.

Table 1. Properties of polypropylene [29]

Properties	Standards	Value	UM
General			
Melt flow index (MFI) (230ºC/2,16kg)	ISO 1133	25	g/10min
Density	ISO 1183	0,900	g/cm^3
Thermal			
Vicat Softening Temperature (Condition A120)	ISO 306	150	ºC
Mechanical			
Tensile Stress at Yield	ASTM D638	33	MPa
Charpy Impact Strength (23°C / Notched)	ISO 179	2,5	kJ/m^2
Flexural Modulus	ISO 178	1400	MPa

-$Fe_{12}SrO_{19}$ powder filling - from the company TODA Ferrite, Korea with the properties presented in Table 2 [30].

Table 2. Properties of $Fe_{12}SrO_{19}$ powder [30]

Property Name	Property Value
Molecular Weight	1061.7
Melting point	> 450°C (lit.)
Density	5.18 g/ mL at 25°C (lit.)
Solubility	Soluble in organic solvents

-Filler - F1 type $Fe_{12}SrO_{19}$ concentrate granules with coding HM 1213 -PA12 + 85% $Fe_{12}SrO_{19}$ - company Mate Co. Ltd [31]; the properties are presented in Table 3.

Table 3. Properties of $Fe_{12}SrO_{19}$ granular concentrate, type F1[31]

Properties	Type F1-HM 1213-PA12+85% $Fe_{12}SrO_{19}$
Specific gravity	3.2 g/cm^3
Melting point	190 ºC
Residual magnetic field strength	235 mT
Coercive force	177 kA/m
Intrinsic coercive force	251 kA/m
Maximum stored energy	10.9 kJ/m^3
Density after ripening	3.21 g/cm^3
Flow index at 270ºC/10 kg	130 g/10 min
Resistance to bending	125 MPa
Impact resistance	28 kJ/m^2

Obtaining the composite materials consisted in the mechanical mixing and primary homogenization in the polymer mass of the percentages established of filler from ferrite powder/ferrite concentrate, followed by the introduction of the mixture thus formed, on the machine screw of injection from melt according to [32]. The processing temperatures of these materials are in the range of 180 - 250°C, and the working pressure is in the range of 138-155 kN being used to achieve disc-shaped materials with a diameter of 30 ± 0.1 mm and a thickness of 2 ± 0.1 mm. The concentrations of the obtained composite materials, as well as their coding, are presented in Table 4 and Figure 1.

Table 4. Sample composition and coding

Composite material	Composition (%) PP/ $Fe_{12}SrO_{19}$	Composition (%) PP/concentrated of $Fe_{12}SrO_{19}$
M0	100/0	
M1	75/25	
M2	70/30	
M3		75/25
M4		70/30

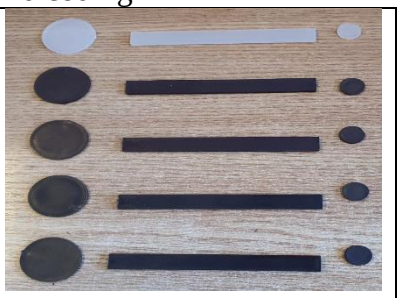

Figure 1. Obtained composites materials

The composites with the maximum percentage of filler were also aged for 168 h at 65ºC to identify the changes occurring in the thermal degradation process. FTIR and UV-Vis tests were performed on these aged samples.

2.1. Equipment and method

The obtaining and characterization of these materials was carried out with the following equipment: a mechanical mixing device/turbine and a melt injection machine Dr. Boy 35 A- Germany [32].

For the composites characterization, various devices were used depending on the determinations made:

• The hydrostatic density was determined with the XS204 Analytical Balance, precision: 0.1mg; linearity: ± 0.2mg; density kit for solids and liquids;

To perform these tests, the applied procedure was according to ASTM D792-20 [33].

The working temperature was 22°C (ambient). The density was determined as the mean value between 4 measurements performed on 4 different samples. Density of the composites obtained by injection from the melt was determined by the Archimedes method, on 4 cylindrical samples, 30 mm in diameter and 2 mm in height.

• The determination of resistance to the action of water was carried out with the XS204 analytical balance, precision: 0.1mg; linearity: ± 0.2mg and a *Memmert* oven;

The effectiveness of an electromagnetic shield can be affected by various factors, including exposure to water. There are several ways in which water could potentially affect the functionality and integrity of an electromagnetic shield: *corrosion- exposure to water can lead to rusting or oxidation. This process weakens the material and may compromise its ability to effectively block electromagnetic radiation; *conductivity: Water could potentially interfere with the shield's ability to direct electrical current. This would only be significant if water were able to penetrate or come into contact with the conductive layer(s) within the shielding material; *structural integrity: exposure to water could compromise the structural integrity of shielding material (if its composed of multiple layers) by causing swelling, delamination, or other forms of degradation, which might result in gaps or openings within the shield that would allow electromagnetic radiation to penetrate and affect electronic devices inside.

Thus, to maintain the effectiveness of an electromagnetic shield in a water-exposed environment, it is essential that the material is corrosion-resistant, minimizes the risk of structural degradation due to exposure to moisture, and prevents contaminants from entering or affecting its integrity. Therefore, the polymer material obtained is waterproof and without cumulative effect for water conductivity.

Water absorption determination tests are performed according to ISO 62:2008 (EN) point 6.4 method 2 [34] on 3 samples from each experimental composite model with a 24h test cycle.

Tests were carried out at 4 test cycles, respectively 24h, 48 h, 96h and 192h. The following formulas are used to calculate the amount of water absorbed (in %):

$$c = \frac{m_2 - m_1}{m_1} x100\% \quad (1)$$

where:

c - amount of water absorbed (%)

m_1 - sample mass (mg) dry, before immersion,

m_2 - sample mass (mg) after immersion

The magnetic tests consisted of carrying out the comparative hysteresis cycle for M2 and M4 (materials with a 30% filler concentration) and the tests to determine the magnetic permeability.

Each sample was prepared as a hollow cylinder having an external diameter of 20 ± 0.1 mm, an internal diameter of 16 ± 0.1 mm, and a thickness of 2 ± 0.1 mm to measure the inductance at the ends of the wire. When the cylindrical sample is inserted into the Test Fixture kit, an ideal, single-turn inductor, with no flux leakage, is formed. Permeability is derived from the inductance of the core with the fixture. The real (μ′) and imaginary parts (μ″) of magnetic permeability were determined from the inductance measurements over the frequency range of 8-30 MHz, according to following equations [35, 36].

$$\mu' = \frac{lL_{eff}}{\mu_0 N^2 A} \quad (2)$$

$$\mu'' = \frac{l(R_{eff} - R_w)}{\mu_0 N^2 \omega A} \quad (3)$$

where: l is the average length of the magnetic core, L_{eff} is the coil inductance, R_{eff} is the equivalent resistance of the magnetic core losses including the wire resistance, N is the number of windings, R_w is the wire resistance, A is the cross-sectional area of the magnetic core,ω is the angular frequency (ω = 2πf), f is the linear frequency (Hz), and μ_0 is the permeability of vacuum ($\mu_0 = 4\pi \times 10^{-7}$ H/m).

The total efficiency of the electromagnetic shielding of samples with a thickness of approx. 2 mm is given by the sum between reflection and absorption (4) [35, 36].

$$SE = SE_R + SE_A \quad (4)$$

The reflection shielding efficiency is given by formula (5)

$$SE_R(dB) = 10\log\left(\frac{\sigma_{AC}}{16\omega\mu_r\varepsilon_0}\right) \quad (5)$$

$$SE_R(dB) = 20\frac{d}{\delta}\log e = 20d\sqrt{\frac{\mu_r\,\omega\sigma_{AC}}{2}}x\log e \quad (6)$$

where:

d - the thickness of the screen (in m) representing the depth with which the radiation penetrates the material,

SE_A - absorption shielding efficiency,

SE_R - reflection shielding efficiency,

μ_r - real magnetic permeability,

ε_r - real permittivity

tg δ - dielectric loss

log *e* - propagation term used in logarithmic function for the adsorption loss calculation

$$\sigma = 2\pi f\varepsilon_o\varepsilon_r tg\delta \quad (7)$$

Substituting results [36]:

To estimate the shielding efficiency, we used formula 8.

$$SE(dB) \approx 10\log(\frac{\sigma}{16\omega\varepsilon}) + 20\log ed\sqrt{\frac{\omega\mu\sigma}{2}} \quad (8)$$

• The magnetic characterization was carried out on a VSM-7304 Lake Shore vibrating sample magnetometer (VSM);

• Magnetic permeability was determined with an impedance analyzer type 4294A (Agilent technology, Japan, Ltd.) equipped with a 16454A magnetic property measurement kit;

• FTIR analyzes were performed with a JASCO FTIR 4200 spectrometer (Jasco inc., JP) [37] equipped with an ATR (Attenuated Total Reflection) PRO470H device, at a resolution of 4 cm^{-1}, in the spectral range 400-4000 cm^{-1}, 100 accumulations/spectrum;

• UV-Vis analyzes were performed with the Jasco V-570 spectrometer (Jasco inc., JP) [38];

• The dielectric characterization was carried out with the help of the dielectric spectrometer Solartron Analytical, UK [39];

• ESDI functional tests were performed with the Novocontrol measuring device.

3. Results and discussions

3.1. Determination of hydrostatic density

From the experimental data obtained as a result of these tests, it can be seen that the densities of the composites are quite close due to the very close concentrations of the filler. However, the highest values are presented by the composites coded with M2 and M4. This can be explained by the fact that they have the highest concentration of the filler ($Fe_{12}SrO_{19}$ powder and $Fe_{12}SrO_{19}$ concentrate granules), respectively 30%. According to them, the composites with concentrations of 25% of the filler respectively M1 and M3 and, as expected, the natural polymer M0 have the lowest densities.

The experimental data were presented in Table 5 and Figure 2.

Table 5. Classification of composites according to density

Code	Density ± std. dev. (g/cm³)	
M0	0.89	0.0022
M1	1.077	0.0015
M2	1.157	0.0019
M3	1.068	0.019
M4	1.157	0.0013

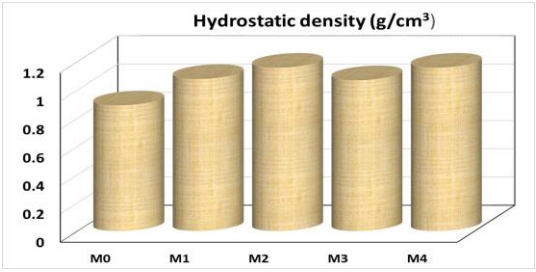

Figure 2. Hydrostatic density

3.2. Water absorption

The amount of water absorbed by the composite materials studied were analyzed by comparison with the control, namely natural polypropylene (M0).

Table 6 shows the absorption of these materials (WA) as a function of time.

The experimental results obtained for water absorption were presented in Figure 3.

Table 6. Water absorption of composites (%)

Code	WA 24h (%)	WA 48h (%)	WA 96h (%)	WA 192h (%)
M0	0.0091	0.0122	0.0244	0.0244
M1	0.0073	0.0223	0.0339	0.0363
M2	0.0105	0.0143	0.0258	0.0344
M3	0.0103	0.0284	0.0438	0.049
M4	0.0072	0.0264	0.0479	0.0551

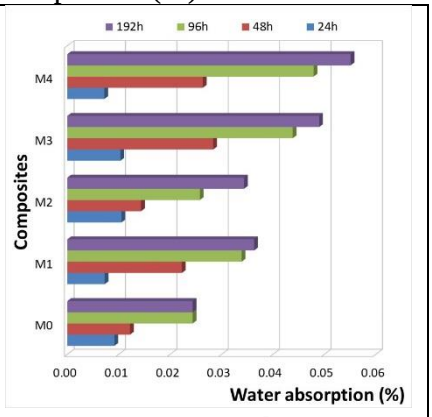

Figure 3. Water absorption

The insignificant water absorption by the composite is mainly due to the fact that the strontium ferrite filler contains -OH functions that form hydrogen bonds with water. From these tests it is found that in the case of composites made with fillers from $Fe_{12}SrO_{19}$ concentrate granules (M3 and M4) the water absorption is somewhat higher than in the case of composites with only $Fe_{12}SrO_{19}$ powder filler (M1 and M2). This can be explained by the fact that in the process of homogenization in the melt of the polymer with the two types of fillers (powder and concentrate) in the case of the concentrate, the polymer that constitutes the shell of the concentrate granule (respectively PA12) intervenes in the mixture and between them certain phenomena at the interface appear, thus creating more voids compared to the polymer blend with only $Fe_{12}SrO_{19}$ powder. These voids allow for faster water absorption.

The water adsorption values recorded for both the ferrite powder and the concentrate even after 192 h are insignificant. This aspect proves a good resistance of the electromagnetic shielding effect of these polymer composites to the action of water.

3.3. FTIR analyses

FTIR spectra were recorded on the primary ferrite and on neat PP polymer samples (Figure 4).

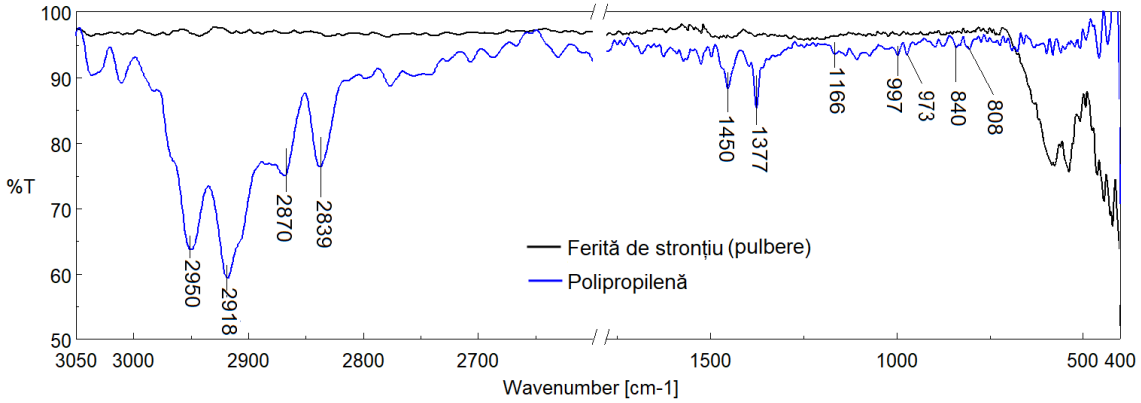

Figure 4. Comparative FTIR spectra recorded on primary ferrite and neat PP polymer samples

Figure 5 shows the spectra recorded on the PP/$Fe_{12}SrO_{19}$ polymer composites (M1-M4).

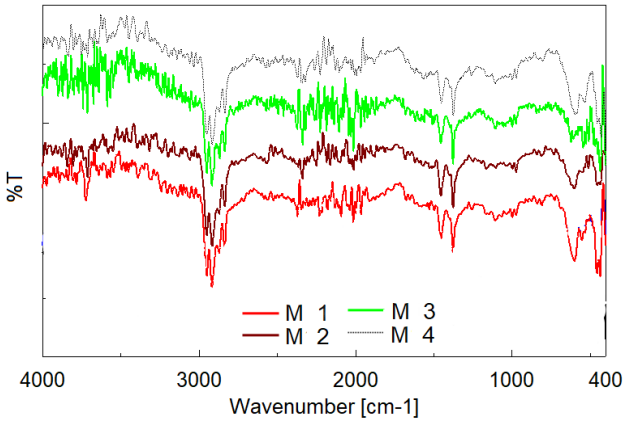

Figure 5. Comparative FTIR spectra recorded on the obtained polymer composites

For M3, the sample obtained was studied in comparison with the one subjected to heat treatment (aged sample) for 168 h/ 65°C (Figure 6).

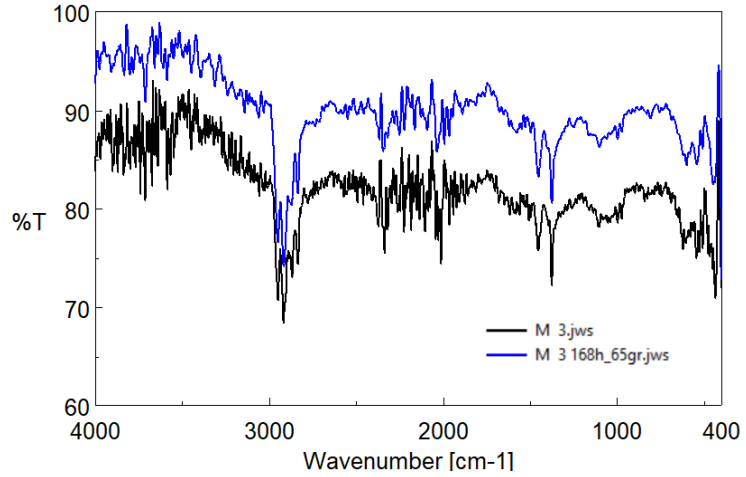

Figure 6. Comparison of FTIR spectra for initial and thermally aged samples

The recorded FTIR spectra (Figure 4-6) show characteristic bands of the analyzed materials.

Polypropylene (PP) shows specific maxima at: 2950 cm^{-1} (CH_3 asymmetric stretching), 2918 cm^{-1} (CH_2 asymmetric stretching), 2870 cm^{-1} (CH_3 stretching), 2839 cm^{-1} (CH_2 stretching) [40, 41], 1450cm^{-1} and 1377 cm^{-1} (CH_3 symmetric bending), 1166 cm^{-1} (C-H and CH_3), 997 cm^{-1} (C-C and CH_3), 973cm^{-1} (C-C and CH_3), 840 (C-H) and 808 (C-C) cm^{-1}. Strontium ferrite shows FTIR maxima [39] in the low frequency spectral range at 580 cm^{-1} and 539 cm^{-1} characteristics of Fe-O and Sr-O tetrahedral bonds, respectively at 428 cm^{-1} and 442 cm^{-1}, characteristic of octahedral bonds Fe-O and Sr-O.

The FTIR spectra recorded on the strontium ferrite granules (Figure 4) show, in addition to the characteristic peaks of ferrite (428 cm^{-1} and 580 cm^{-1}) also the characteristic peaks of the powder coating matrix with bands characteristic of polyamide [42-46]. The FTIR spectra recorded on the PP/$Fe_{12}SrO_{19}$ composite samples (Figure 5) show all the characteristic bands above, no major spectral changes being highlighted. However, depending on the added ferrite concentration, a variation in the intensity of the characteristic ferrite peaks (428 cm^{-1} and 580 cm^{-1}) is observed. Exposure to an external stress factor (such as temperature) did not show spectral changes suggesting certain degradation of the material structure (Figure 6).

3.4. UV-Vis analyses

The experimental results obtained from these analyzes are presented in Figure 7.

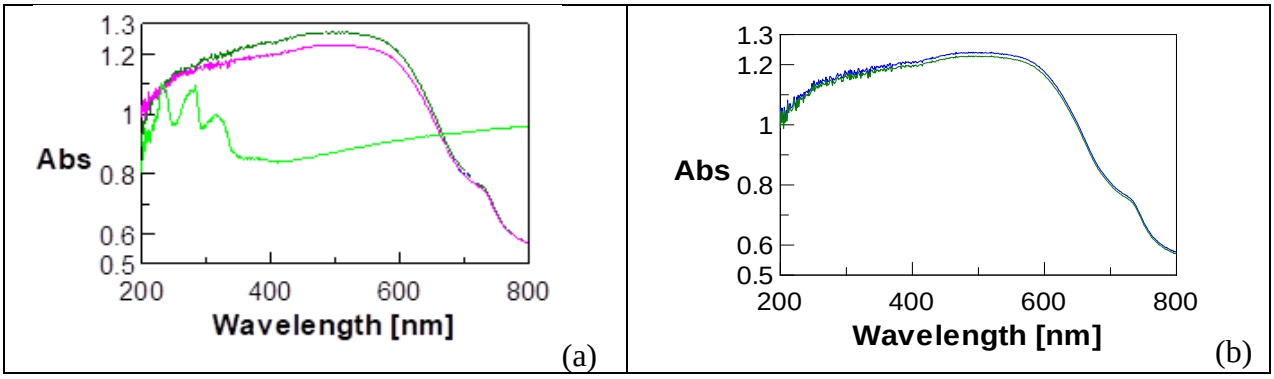

Figure 7. UV-Vis spectra for (a) the non-thermally treated composites M0 - green, M1 - black and M2 - pink and (b) the thermally treated composites (thermally aged samples) 168 h at 65°C M2 - red and M4 - blue

The samples of composite materials, based on PP/filler ($Fe_{12}SrO_{19}$ powder/ $Fe_{12}SrO_{19}$ concentrate granules) analyzed, show broad absorption maximum values with a plateau between 500-600 nm and absorbance around 1.3 arbitrary units. The appearance of the UV-Vis spectra indicates the homogeneity of the samples obtained with the functional filler of strontium ferrite.

Ageing the samples with temperature (168 h/65°C) resulted in minor changes in the UV-Vis spectrum.

In conclusion, ageing for 168 h at 65°C does not lead to perceptible changes.

3.5. Dielectric tests

Dielectric tests were performed in the range 10 kHz - 8 MHz for the classification of composite materials in terms of electrical conductivity, which is calculated using formula (6).

Figure 8 shows the variations of tg δ and σ for the studied composite materials.

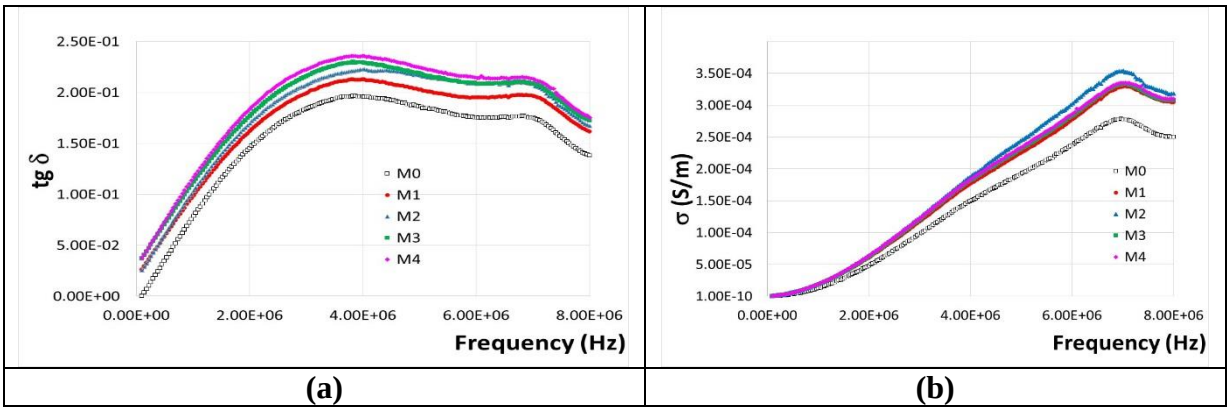

(a) **(b)**

Figure 8. Variations of (a) tg δ and (b) σ with frequency of the analyzed composite materials

From the comparative analysis of the obtained experimental data related to tg δ for the composite materials with fillers compared to the natural polymer, it can be said that the addition of fillers leads to an increase in dielectric losses and at the same time in electrical conductivity.

Table 7 shows the percentage increase in tg δ and σ values compared to the natural polymer (M0).

Table 7. Variations of tg δ and σ, relative to the natural polymer (M0)

% increase compared to M0	tg δ M1	σ M1	tg δ M2	σ M2	tg δ M3	σ M3	tg δ M4	σ M4
	10.92	15.86	15.43	21.69	17.79	17.54	20.16	18.60

It is found that the composites with the highest percentage of $Fe_{12}SrO_{19}$ and M2 powder respectively (It is found that the composites with the highest percentage of $Fe_{12}SrO_{19}$ and M2 powder respectively (about 22%) show the greatest increases in electrical conductivity. If one analyzes the increase in electrical conductivity of the composites relative to the PP polymer matrix, it can be said that, when adding 30% ferrite, σ_{M2} increases with about 22% relative to σ_{PP}, while σ_{M4} increases with about 19% relative to σ_{PP}. This can be justified by the fact that in the $Fe_{12}SrO_{19}$ concentrate there is a small amount of PA12, used in ferrite powder encapsulation.

3.6. Magnetic tests

3.6.1. The hysteresis cycles (Figure 9) were performed on samples with maximum filler concentration (e.g., M2 and M4). These indicate that at the same percentage of added ferrite, Sr ferrite powder provides a higher magnetic moment than ferrite concentrate. It should also be noted that no sample reached magnetic saturation.

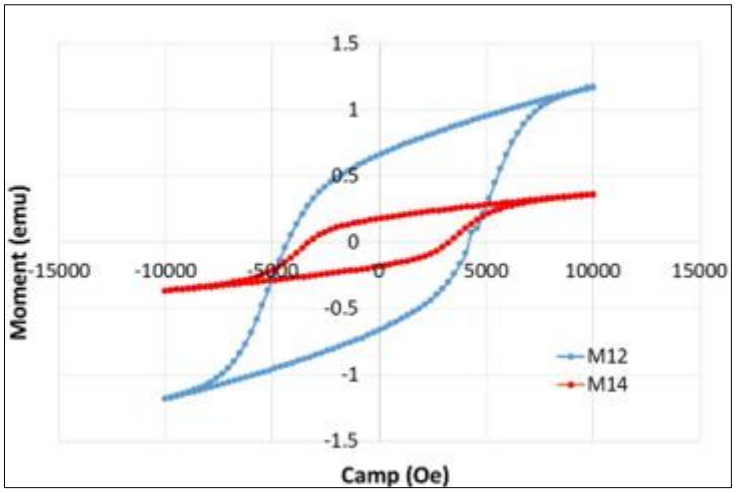

Figure 9. Hysteresis cycle for M2 and M4

3.6.2. The estimation of the electromagnetic shielding efficiency was calculated with the help of formulas 3-8 using the magnetic permeability values. For the analyzed electromagnetic materials, the magnetic permeability was determined in the range of 40Hz - 25MHz. Figure 10 shows the variation of magnetic permeability with frequency in alternating current of composite materials M0-M4 with maximum ferrite concentration.

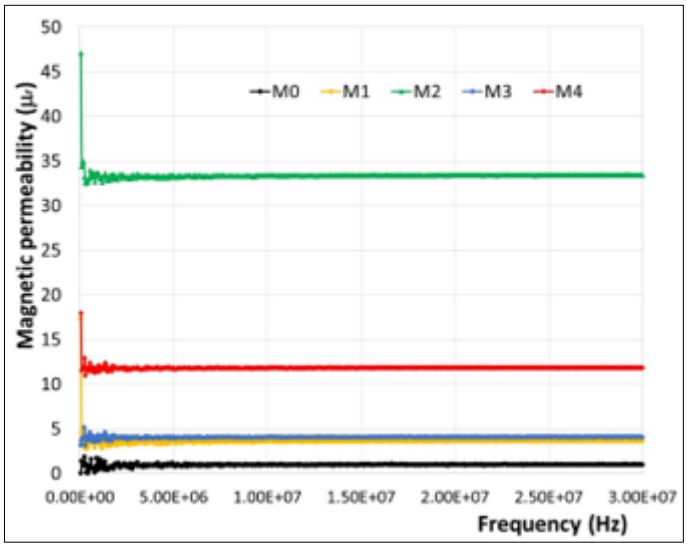

Figure 10. Variation of magnetic permeability for composite materials M1- M4

It is found that the materials with maximum percentage of filler (respectively 30%) have the highest magnetic permeability, as shown in Figure 10.

The experimental values of the magnetic permeabilities allowed the calculation of SE reflection and SE absorption using formula 8.

It is found that for these materials, up to 30 MHz there is shielding by reflection (SE_R) and a very small shielding by absorption (SE_A), this being almost negligible.

This can be explained by the fact that absorption shielding also depends on the thickness of the samples, which is very small, between 1.9 - 2.75 mm. The variation of the reflection shielding efficiency (SE_R) and absorption shielding efficiency (SE_A) with the frequency for the M1-M4 composite materials is shown in Figure 11.

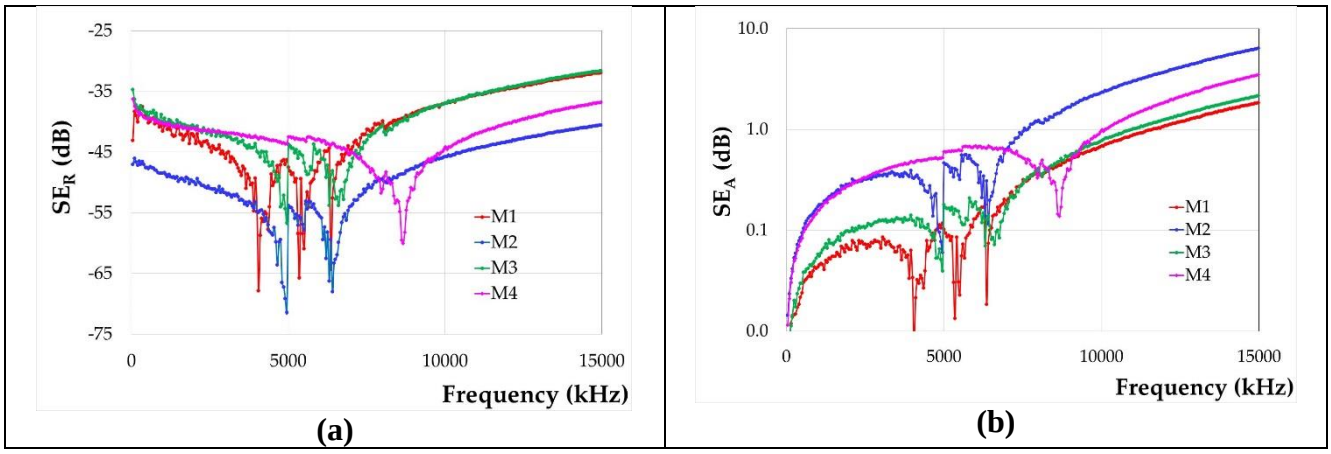

Figure 11. a) Reflection shielding efficiency (SE_R) and b) absorption shielding efficiency (SE_A) for the M1-M4 composite materials

The maximum values of the SE_R and SE_A for the analyzed materials are summarized in Table 8.

Table 8. Maximum values of SE_R and SE_A for the M1-M4 composite materials

Sample code	SE_R (dB)	SE_A (dB)	Frequency (Hz)	$SrFe_{12}O_{19}$ powder/concentrate content (wt.%)
M1	−67.8	0.01	4.05E+06	25
M2	−71.5	0.06	6.58E+06	30
M3	−56.7	0.04	4.96E+06	25
M4	−60.1	0.14	8.66E+06	30

In Table 8 one can notice that the M2 material has the highest reflection shielding efficiency (SE_R) among the analyzed materials. If we compare the SE_R results for the M1 and M2 materials made with $SrFe_{12}O_{19}$ powder filler, it is found that an increase in filler concentration from 25 to 30 wt.% leads to an increase in the SE_R value by about 11%, while for the M3 and M4 materials with $SrFe_{12}O_{19}$ concentrate, an increase of about 6% is observed. This means that the powder leads to better shielding properties. The values for the same concentration samples (M4-M2 composites with 30% concentration and M3-M1 with 25% concentration) recorded maximum reflection SE of about 76 % for M4 relative to M2 and about 82 % for M3 relative to M1.

This is explained by the fact that when obtaining composites using $SrFe_{12}O_{19}$ concentrate as a filler (M3 and M4), homogenization with the polypropylene (PP) polymer matrix is hampered by the polyamide (PA) existent in the F1-type ferrite concentrate, which is not miscible with polypropylene and during rheological mixing in the melt creates repulsive forces that lead to the appearance of defects, resulting in a decrease in reflection SE.

3.7. ESD functional tests

Testing of the ESD properties of the composites was carried out in an accredited Renar EMC-EMI laboratory of the Technical University of Iași with up-to-date calibrated equipment.

Tested:

- Surface resistance Rs according to Standard Test EN 61340-2-3
- Point-to-point resistance Rp according to Standard Test EN 61340-5-1

The minimum requirements for materials usable as protection against electrostatic discharges are:

- Surface resistance Rs maximum 106-108 Ω x m [47]
- Point to point resistance Rp 104 - 1010 Ω [48]

The experimental results obtained are presented in Table 9.

Table 9. Comparative dielectric and ESD data

Code	10Hz permittivity	ΔTg 10 Hz	Surface resistance Rs	Point to point resistance Rp
M0	2.25	10^{-4}	10^{14}	10^{16}
M1	3.46	$1.75x10^{-2}$	$2.2x10^{7}$	$4x10^{9}$
M2	3.73	$2.7x10^{-2}$	$1.2x10^{7}$	$2x10^{9}$
M3	3.19	$1.4x10^{-2}$	$9.5x10^{7}$	$4x10^{10}$
M4	3.31	$2x10^{-2}$	$7x10^{7}$	$2x10^{10}$

Composites recommended for simultaneous EMI and ESD functionality are in order of their performance, namely: M2 (with 30% ferrite powder) and then M1 (with 25% ferrite powder). The M4 composite (with 30% ferrite concentrate) which has surface resistivity and point resistance very close to the imposed value can also be used at the limit.

4. Conclusions

In this work, 5 experimental models of PP/$Fe_{12}SrO_{19}$ polymer composite materials with mass concentrations of 100/0, 75/25 and 70/30 and coding M0-M4 were obtained by melt injection and characterized. Strontium ferrite ($Fe_{12}SrO_{19}$) was used in powder form for samples M1 and M2 and concentrate for samples M3 and M4. Among these, those that show performance in simultaneous applications in protection against electrostatic discharges and electromagnetic pulses were chosen. The determined values analysis and the characterization of the obtained polymer materials was carried out based on the results of the experimental tests performed.

Following these characterizations, the composite coded with M2 with the composition PP/$Fe_{12}SrO_{19}$ in a concentration of 70/30 was chosen as the optimal variant. By comparing the behavior of powder and granule type composite materials, it is found that those obtained using ferrite concentrate are more homogeneous but present lower SE_R values than those with ferrite powder filler. All the samples of composite mixtures based on ferrite presented insignificant values regarding the degree of water adsorption. This shows that they have a good stability to the action of water, therefore a good resistance to both the electromagnetic shielding effect and the electrostatic transfer of the materials.

The paper concludes with functional tests for ESD and EMI applications. For these applications, the surface resistance Rs and the point-to-point resistance Rp were tested. The composites recommended for simultaneous EMI and ESD functionalities in the order of their performance are samples M2 (with 30% ferrite powder), M1 (with 25% ferrite powder) and at the limit the composite M4 (with 30% concentrate with ferrite powder) which presents characteristics (surface resistivity and point resistance very) close to the imposed value.

The final conclusion of the obtained experimental results demonstrates that composites with superior simultaneous EMI and ESD shielding properties can be made. The advantages of these composites are:

- can be carried out on a large scale,
- are cheap,
- have ferritic powder type filling in minimum concentration, and
- they are easy-to-process thermoplastic materials for applications in the electrotechnical, electronics and automotive industries.

Acknowledgments: This work was supported by Romanian Ministry of Research, Innovation and Digitalization, project number 25PFE/30.12.2021-Increasing R-D-I capacity for electrical engineering-specific materials and equipment with reference to electromobility and “green” technologies within PNCDI III, Programme 1 and project number PN23140201-42N/2023, carried out within National Institute for Research and Development in Electrical Engineering ICPE—CA Bucharest.

References

1. BHATTACHARJEE, P.K., Universal law of gravitation compares with electromagnetic waves propagation, *IOSR Journal of Electronics and Communication Engineering*, 14, 2019, 44-48. https://doi.org/10.9790/2834-1403024448
2. BHATTACHARJEE, P.K., Fundamental to electromagnetic waves, *International Journal of Trend in Scientific Research and Development*, 7, 2023, 454-462.
3. BHATTACHARJEE, P. K., Mobile phone and system are designed in a novel way to have minimum electromagnetic wave transmission in air and minimum electrical power consumption, *International Journal of Computer Networks and Wireless Communications*, India, 2, 2012, 556-559.
4. DIVAN, S., ROSENCRANZ, A., Environment Law and Policy in India: Cases, Materials and Statutes, Oxford University Press, 23rd Edition, 2021.
5. SUKANTA, K.N., PASAYAT, A., Environmental Law, *Central Law Publication*, Allahabad, India, 5th Edition, 2021.
6. LINGVAY, I., VOINA, A. LINGVAY, C., MATEESCU, C., The impact of the electromagnetic pollution of the environment on the complex build-up media, *Revue Roumaine des Sciences Techniques, Série Électrotechnique et Énergétique*, 53, 2008, 95-111.
7. HOU, Y.-S., LIN, C.-Y., Characterization of ESD-induced electromigration on CMOS metallization in on-chip ESD protection circuit, *Japanese Journal of Applied Physics* 63(2), 2023, DOI: 10.35848/1347-4065/ad1776
8. CARAMITU, A.-R., CIOBANU, R.-C., ION, I., SCHREINER, C., ARADOAEI, M., TSAKIRIS, V., PINTEA, J., MARINESCU, V., Flexible electromagnetic shielding nano-composites based on silicon and $NiFe_2O_4$ powders, *Polymers*, ISSN 2073-4360, 5(11), 2023, 2447. https://doi.org/10.3390/polym15112447, WOS:001005724100001.
9.CARAMITU, A.-R., ION, I., BORS, A.-M., TSAKIRIS, V., PINTEA, J., CARAMITU, A.-M.D., Preparation and spectroscopic characterization of some hybrid composites with electromagnetic shielding properties exposed to different degradation factors, *Mater. Plast.*, **59**(4), 2022, 82-94. https://doi.org/10.37358/MP.22.4.5627, WOS:000965030700007.
10. CARAMITU, A.-R., ION, I., BORS, A.-M., CIOBANU, C.-R., SCHREINER, C., ARADOAEI, M., CARAMITU, A.-M.D., Physico-chemical characterization of paint films with electromagnetic properties, *Mater. Plast.*, **59**(2), 2022, 9-23. https://doi.org/10.37358/MP.22.2.5580, WOS: 000831634900002.
11.BOLTE, F.B.J., BALIATSAS, C., EIKELBOOM, T., IRENE VAN KAMP, Everyday exposure to power frequency magnetic fields and associations with non-specific physical symptoms, *Environmental Pollution*, 196, 2015, 224-229. https://doi.org/10.1016/j.envpol.2014.10.011
12.MASLANYJ, M., SIMPSON, J., ROMAN, E., SCHÜZ, J., Power frequency magnetic fields and risk of childhood leukemia: misclassification of exposure from the use of the 'distance from power line' exposure surrogate, *Bioelectromagnetics*, 30, 2009,183-188. https://doi.org/10.1002/bem.20465
13. BALIATSAS, C., IRENE VAN KAMP, BOLTE, J., SCHIPPER, M., YZERMANS, J., LEBRET, E., Non-specific physical symptoms and electromagnetic field exposure in the general population: can we get more specific? A systematic review, *Environment International*, 41, 2012,15-28. https://doi.org/10.1016/j.envint.2011.12.002
14.SZEMERSZKY, R., ZELENA, D., BARNA, I., BARDOS, G., Stress-related endocrinological and psychopathological effects of short- and long-term 50Hz electromagnetic field exposure in rats, *Brain Research Bulletin*, 81, 2010, 92-99. https://doi.org/10.1016/j.brainresbull.2009.10.015
15.RADU, E., LIPCINSKI, D., TANASE, N., LINGVAY, I., The influence of the 50 Hz electric field on the development and maturation of Aspergillus Niger", *EEA-Electrotehnica, Electronica, Automatizări*, 63, 2015, 68-74.

16.STANCU C., LINGVAY M., SZATMARI I., LINGVAY I., Influence of 50 Hz electromagnetic field on the yeast (saccharomyces cerevisiae) metabolism, *8th International Symposium on Advanced Topics in Electrical Engineering*, Bucharest, 2013, https://doi.org/10.1109/Atee.2013.6563449
17.CARAMITU, A.-R, BUTOI, N., RUS, T., LUCHIAN, A-M., MITREA, S., The resistance to the action of molds of some painting materials aged by thermal cycling and exposed to an electrical field of 50 Hz, *Mater. Plast.*, **54**(2), 2017, 331-337. https://doi.org/10.37358/MP.17.2.4845
18.LINGVAY, M., CARAMITU, A.R., BORS, A.-M., LINGVAY, I., Dielectric spectroscopic evaluation in the extremely low frequency range of an Aspergillus Niger culture, *Studia Universitatis Babes Bolyai, Chemia*, 2(I), 2019, 279-288. https://doi:10.24193/Subbchem.2019.2.23.
19.SANDU, D., LINGVAY, I., SZABOICS, L., MICU, D., POPESCU, C., JURGEN, B., BARTHA, C., CSABA, P., The effect of electromagnetic fields on baker's yeast population dynamics, biocatalytic activity and selectivity, *Studia Universitatis Babes Bolyai. Chemia*, LIV, 4, 2009, 195-201.
20.BARTHA, C., CARAMITU, A.R., JIPA, M., IGNAT, M.D., TOKOS, A., Dielectric behavior of sludge from wastewater treatment, *Studia Universitatis Babes Bolyai, Chemia*, LXV, 4, 2020, 85-93. https://doi:10.24193/Subbchem.2020.4.07
21. TÓKOS, A., BARTHA, C., JIPA, M., MICU, D-D., CARAMITU A.R., LINGVAY, I., Inter-actions of extremely low-frequency electric field with the active sludge live materia from wastewater treatments, *12th International Symposium on Advanced Topics in Electrical Engineering* (ATEE), 2021. https://doi:10.1109/Atee52255.2021.9425187
22.OPESCU, I., STĂNESCU, R., BIASIOLI, M., MARSAN, F.-A., CONSTANTINESCU, I., Assessing human risks through soil exposure model for a soil contamination associated to heavy metals, *U.P.B. Sci. Bull., Series B*, 75(1), 2013, ISSN 1454-2331
23. MIRON, A.-R., MODROGAN, C., ORBULEŢ, O.-D., COSTACHE, C., POPESCU, I., Treatment of acid blue 25 containing wastewaters by electrocoagulation, *U.P.B. Sci. Bull., Series B*, 72(1), 2010, ISSN 1454-2331
24. YAKOVENKO, O.S., MATZUI, L., VOVKENKO, L., LAZARENKO, O., PERETS, Y.S., LOZISKY, O.V., Complex permittivity of polymer-based composites with carbon nanotubes in microwave band, *Applied Nanoscience*, 10, 2020, 2691–2697. https://doi:10.1007/s13204-019-01083-5
25. RADON, A., HAWEŁEK, Ł., ŁUKOWIEC, D., KUBACKI, J., WŁODARCZYK, P., Dielectric and electromagnetic interference shielding properties of high entropy (Zn, Fe, Ni, Mg, Cd) Fe2O4 ferrite, *Scientific Reports*, 9, 2019, 20078. https://doi:10.1038/s41598-019-56586-6
26. SHABZENDEDAR, S., MODARRESI-ALAM, A.R., NOROOZIFAR, M., KERMAN, K., Core-shell nanocomposite of superparamagnetic Fe3O4 nanoparticles with poly (m-amino-benzenesulfonic acid) for polymer solar cells, *Organic Electronics*, 77, 2019, 105462. https:// doi.org/10.1016/J.Orgel.2019.105462.
27. RAHEEM, A.J., MUSTAFA, J.M., Preparation of composite materials of silicon rubber reinforced by (CrMnxNi1-XFeO4) for microwave absorption at X-band, *International Journal of engineering research and technology*, ISSN 0974-3154, 11, 2018, 273-285.
28. HEMEDA, O. M., HENAISH, A.-M.A., SALEM, B.-I., SBAKHY, F.-S.E., MAHMOUD A.-H., The dielectric and magnetic properties of RTV-silicon rubber Ni–Cr ferrite composites, *Applied Physics A*, 126, 2020.https://doi.org/10.1007/s00339-020-3297-y
29. RESINEX PP RXP 2004 NATURAL (PP/25/1300μ), catalog sheet - Polypropylene powder
30.***https://www.chemicalbook.com/ChemicalProductProperty_EN_CB3493555.htm
31.***16-08-17 MATE catalog (EN), version 4
32.***IL MAV – 06/2014 Injection molding machine working instruction, Dr. Boy Germania.
33.***STM D 792-20 Standard test methods for density and specific gravity (Relative Density) of plastics by Displacement
34.***ISO 62/2008 Plastics - Determination of water absorption
35. SIMU, C., MARZA, E. Propagation of electromagnetic waves, book: Radio antennas, University Horizons Publishing House, Timisoara, 2000 https://www.researchgate.net/publication/318494656.

36. HAWAN, S.K., OHLAN, A., SINGH, K., Designing of nano composites of conducting polymers for EMI shielding, book: Advances in nanocomposites - Synthesis, characterization and industrial applications, 2011, 429-482. https://doi.org/10.5772/14752
37.***Spectrometer JASCO FTIR 4200 (Jasco inc., JP) equipped with an ATR (Attenuated Total Reflection) PRO470H device, operating manual
38.***Spectrometer Jasco V-570 Japan, operating manual
39.***IL MAV – 06/2017, operating instructions SOLARTRON dielectric Spectrometer
40.LUNGULESCU, E.M., LINGVAY, I., UNGUREANU, L.C., RUS, T., BORS, A.M., Thermo-oxidative behavior of some paint materials in natural ester based electro-insulating fluid.
Mater. Plast., **55**(2), 2018, 201-206, doi:10.37358/MP.18.2.4995.
41. LUNGULESCU, M.E., ZAHARESCU, T., PLESA, I., PODINA, C., Thermal and radiation stability of polyolefins modified with silica nanoparticles, *J. Optoelectron Adv. M*, 16, 2014, 719-725.
42. ZAHARESCU, T., LUNGULESCU, M.E., CARAMITU, A.R., MARINESCU, V., Study on radiation aging of PA6/EPDM blends, *Polym J*., *Iran*, 2015, 24, 883-889,
doi:10.1007/s13726-015-0376-6.
43.LUNGULESCU, E.-M., Contributions to the study and characterization of degradation processes of the insulating polymeric materials in high-energy radiation fields. PhD thesis, University of Bucharest, 2014.
44.SHAFIGULLIN, L.N., ROMANOVA, N.V., GUMEROV, I.F., GABRAKHMANOV, A.T., SARIMOV, D.R., Thermal properties of polypropylene and polyethylene blends (PP/LDPE), *IOP Conf., Series: Materials Science and Engineering*, 412, 2018, 012070.
https://doi:10.1088/1757-899X/412/1/012070.
45. KUMAR, S.S., SINGH, R.K., KUMAR, N., KUMAR, G., SHANKAR, U., Structural, elastic, and multiferroic property of strontium ferrite nanoceramic prepared by sol–gel derived citrate precursor method, *Materials Today*, 46, 2021, 8567-8572 https://doi.org/10.1016/j.matpr.2021.03.547.
46. FANG, J., ZHANG, L., SUTTON D., WANG X., LIN, T., Needleless melt-electrospinning of polypropylene nanofibers, *Nanofiber Manufacture, Properties and Applications*, 2012.
https://doi.org/10.1155/2012/382639
47.***Standard test EN 61340-2-3
48.***Standard test EN 61340-5-1

Manuscript received: 12.04.2024